Removal of the airwave effect on MCSEM data by separation of the main part of the anomalous field

Shuming Wang and Michael S. Zhdanov, University of Utah*

Summary

One of the difficulties in interpretation of MCSEM survey data in shallow water is related to the airwave effect, which dominates over the observed EM response and masks the anomalous effect of the resistive target. We demonstrate in this paper that this effect can be practically eliminated by a method of the separation of the main part of the anomalous field. As a result of this separation, the effect of the air-water interface and the seawater layer is completely removed from the transformed signal. The advantage of this technique is that it can be used not only for a flat sea bottom but in areas with rough bathymetry as well. The proposed technique is implemented in the form of a stable integral transformation, which reduces the effect of the noise on the data, while methods based on the interferometry principles require the solution of an ill-posed deconvolution problem. The numerical method of main-part separation is based on the application of corresponding digital filters to the observed data. It is shown that the spectral characteristics of this transformation represent low-frequency filters, which ensures robustness of the numerical algorithm.

Introduction

One of challenging problems of the interpretation of MCSEM data in shallow seas is related to the analysis of the effect of the so-called airwave on the observed data. The airwave represents a direct part of the primary field from the source, which travels from the source to the sea surface and is reflected back to the sea bottom. In a shallow water environment, the amplitude of the airwave exceeds significantly the strength of the response from the sea-bottom reservoir, making interpretation of the MCSEM data a very difficult problem.

During the last several years, several different techniques have been developed to address this problem. One of these techniques is based on upgoing/downgoing separation of the electromagnetic (EM) field (e.g., Amundsen et al., 2006; Zhdanov and Wang, 2009a, 2009b). Another method, which was introduced quite recently, considers the application of an approach similar to seismic interferometry (Fan et al., 2009). Seismic interferometry is a powerful method which has become a subject of intensive research and development during recent years (e.g., Schuster, 2009). It was shown in a number of publications (Sneider, 2006; Amundsen et al., 2006; Slob et al., 2007; Wapenaar et al., 2008) that interferometry can be applied to diffusive fields as well. The main application of interferometry to marine EM is to reduce the airwave effect (Fan et al., 2009). The idea is that, by solving the corresponding interferometry deconvolution problem, one can remove the media above the receivers and, correspondingly, the airwave associated with the air-water interface.

In this paper we demonstrate that exactly the same result can be achieved by a method of separating the main part of the anomalous EM field, introduced by Berdichevsky and Zhdanov (1984). The advantage of this technique is that it can be used not only for a flat sea bottom but in areas with rough bathymetry as well. In addition, the proposed technique is implemented in the form of a stable integral transformation, which reduces the effect of noise on the data, while methods based on the interferometry principles require the solution of an ill-posed deconvolution problem.

Determination of the main part of the anomalous field

The method of upgoing/downgoing EM field separation is widely used now for suppression of the airwave effect on MCSEM data. In an upgoing electromagnetic field, however, the primary effect of the target (HC reservoir) merges with the secondary effect of the surrounding medium formed by the sea surface, seawater layer, and sea-bottom sediments. In order to remove the sea surface and sea bottom effect, one can use the method of separation of the main part of the anomalous field (Berdichevsky and Zhdanov, 1984; Zhdanova and Zhdanov, 1999).

Let us consider a typical MCSEM survey conducted in an area with rough bathymetry described by surface *S*. The conductivity of seawater is known: it is equal to σ_w. Sea-bottom formations are characterized by 3D distribution of the conductivity, $\sigma(\mathbf{r}) = \sigma_b + \Delta\sigma(\mathbf{r})$, where σ_b is a background conductivity of the sea-bottom sediments; $\Delta\sigma(\mathbf{r})$ is an anomalous conductivity of the domain *D* containing local inhomogeneities (e.g., an HC reservoir). We assume that inhomogeneous domain *D* is located within homogeneous or weakly heterogeneous layers of the sea-bottom sediments. The frequency domain EM field is generated by an electric bipole transmitter T_x located at some depth within the seawater layer. This field is measured by a system of receivers located at the sea bottom.

We can represent the EM field in this model as a sum of two components, $\{\mathbf{E}^b, \mathbf{H}^b\}$ and $\{\mathbf{E}^M, \mathbf{H}^M\}$:

$$\mathbf{E} = \mathbf{E}^b + \mathbf{E}^M, \quad \mathbf{H} = \mathbf{H}^b + \mathbf{H}^M, \tag{1}$$

where $\{\mathbf{E}^b, \mathbf{H}^b\}$ is a background EM field generated in the model with the background conductivity σ_b, and $\{\mathbf{E}^M, \mathbf{H}^M\}$ is a field, which satisfies the following equations:

$$\nabla \times \mathbf{H}^M = \sigma_b \mathbf{E}^M + \mathbf{j}^\Delta, \quad \nabla \times \mathbf{E}^M = i\omega\mu_0 \mathbf{H}^M, \tag{2}$$

where

$$\mathbf{j}^\Delta = \mathbf{j}^\Delta(\mathbf{r}) = \Delta\sigma(\mathbf{r})\mathbf{E}(\mathbf{r}), \ \mathbf{r} \in D \tag{3}$$

is the density of the excess current distributed over the inhomogeneity D.

The last formula shows that the field $\{\mathbf{E}^M, \mathbf{H}^M\}$ can be treated as a field excited by the excess current of the density $\mathbf{j}^\Delta$ in a boundless medium with the background conductivity σ_b. This field is called the *main part of the anomalous EM field* (Berdichevsky and Zhdanov, 1984; Zhdanova and Zhdanov, 1999). In the field $\{\mathbf{E}^M, \mathbf{H}^M\}$ the sea surface and the sea floor manifest themselves only inasmuch as they affect a distribution of the current in inhomogeneity $\mathbf{j}^\Delta$. That is why this field is very well suited to study the anomalous field from a sea-bottom reservoir with the distortion effects removed from the seawater layer and from the air-water interface on the MCSEM data.

Separation of the main part of the anomalous field

We use a method based on the Stratton-Chu type integrals (Zhdanov, 1988) to solve a problem of the separation of the main part of the anomalous field. Let us introduce an auxiliary surface S_e, which is obtained by shifting the surface S down along the z axis at some small distance e, so that this auxiliary surface is located entirely within the sediment layer with the conductivity σ_b. The recalculation of the observed data from surface S, located within the seawater, to the auxiliary surface S_e, located within the sea-bottom sediments, can always be achieved by applying the corresponding boundary conditions.

We assume now that the observed EM field is given at the surface, S_e. In this case, the main part of the anomalous field is equal to the upgoing part of the EM field within a medium with background conductivity σ_b. Therefore, we can apply a conventional method of field separation into upgoing/downgoing parts (e.g., Zhdanov and Wang, 2009a, 2009b) using Stratton-Chu type integrals.

According to this method, the main part of the anomalous field is equal to:

$$\mathbf{E}^M(\mathbf{r}') = C^E_{S_e}(\mathbf{r}'), \tag{4}$$

$$\mathbf{H}^M(\mathbf{r}') = C^H_{S_e}(\mathbf{r}'). \tag{5}$$

Here $C^E_{S_e}$ and $C^H_{S_e}$ are the corresponding Stratton-Chu type integrals over surface S_e:

$$C^E_{S_e}(\mathbf{r}') = \iint_{S_e} [(\mathrm{n}\cdot\mathrm{E})\nabla G_b + (\mathrm{n}\times\mathrm{E})\times\nabla G_b + i\omega\mu(\mathrm{n}\times\mathrm{H})G_b]ds, \tag{6}$$

and

$$C^H_{S_e}(\mathbf{r}') = \iint_{S_e} [(\mathrm{n}\cdot\mathrm{H})\nabla G_b + (\mathrm{n}\times\mathrm{H})\times\nabla G_b + \sigma_b(\mathrm{n}\times\mathrm{E})G_b]ds, \tag{7}$$

where $\mathbf{n}$ is the unit vector of an upward pointing normal, and G_b is the fundamental Green's function for the Helmholtz equation in a homogeneous full space with the seawater conductivity σ_b:

$$G_b(\mathrm{r}'|\mathrm{r}) = -\frac{1}{4\pi|\mathrm{r}-\mathrm{r}'|}\exp(ik_b|\mathrm{r}-\mathrm{r}'|), \ k_b = \sqrt{i\omega\mu_0\sigma_b}, \ \mathrm{Re}k_b > 0. \tag{8}$$

Formulas (4) and (5) provide a general solution for a separation of the main part of the anomalous field from the CSEM data given on an observational surface of arbitrary shape. Note that the main part of the anomalous field, according to the definition, is a field generated in the full space with the conductivity σ_b by the excess current $\mathbf{j}^\Delta$, distributed within the inhomogeneity D.

Constructing a digital filter for EM field separation

Formulas (4) and (5) describe a linear transformation of the observed field data. This transformation can be implemented using a digital filter. As an example, let us consider a case where S_e is a horizontal plane.

We can write formulas (4) - (5) in numerical dressings as follows:

$$E^M_x(\mathbf{r}') = \sum_{i=1}^{I}\sum_{k=1}^{K}\left(E_x G_{,z} + E_z G_{,x} - \frac{k_b^2}{\sigma_b} H_y G\right)\Delta x \Delta y,$$
$$E^M_y(\mathbf{r}') = \sum_{i=1}^{I}\sum_{k=1}^{K}\left(E_y G_{,z} + E_z G_{,y} + \frac{k_b^2}{\sigma_b} H_x G\right)\Delta x \Delta y, \tag{9}$$
$$E^M_z(\mathbf{r}') = \sum_{i=1}^{I}\sum_{k=1}^{K}\left(E_z G_{,z} - E_x G_{,x} - E_y G_{,y}\right)\Delta x \Delta y,$$

$$H^M_x(\mathbf{r}') = \sum_{i=1}^{I}\sum_{k=1}^{K}\left(H_x G_{,z} + H_z G_{,x} - \sigma_b E_y G\right)\Delta x \Delta y,$$
$$H^M_y(\mathbf{r}') = \sum_{i=1}^{I}\sum_{k=1}^{K}\left(H_y G_{,z} + H_z G_{,y} + \sigma_b E_x G\right)\Delta x \Delta y, \tag{10}$$
$$H^M_z(\mathbf{r}') = \sum_{i=1}^{I}\sum_{k=1}^{K}\left(H_z G_{,z} - H_x G_{,x} - H_y G_{,y}\right)\Delta x \Delta y,$$

where Green's function G is given by formula (8).

It is important to study the spectral characteristic of the digital filter which may serve as a useful indication of the accuracy of the filter. To check the accuracy, we will compare the spectral characteristic of our digital filter with the analytical characteristic.

As an example, we present the spectral characteristic of a digital filter for one of the field components with the frequency f = 0.5 Hz, horizontal steps $\Delta x = \Delta y$ equal to 30 m, and a vertical step, $\Delta z = z'$, equal to 100 m. The window sizes are equal to $w_x = w_y$ = 6000 m. Taking into account a cylindrical symmetry of the spectral characteristic with respect to the origin of the coordinate plane of the spatial frequencies, k_x and k_y, we show all the results as 2D plots comparing the spectral characteristic of the digital filter with the analytical spectral characteristic along the k_x axis ($k_y = 0$). We show both the real (top panel) and imaginary (bottom panel) parts of the spectral characteristic of the filter.

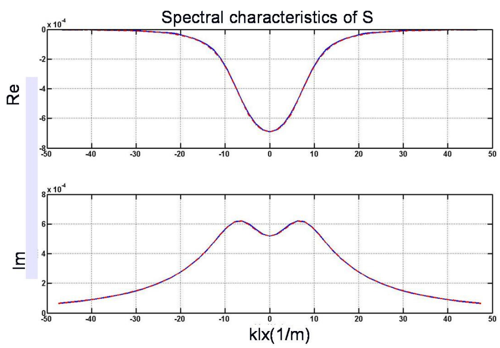

Figure 1: Comparison of the spectral characteristic of a digital filter with the analytical spectral characteristic for the following parameters: $f = 0.5$ Hz; $\Delta x = \Delta y = 30$ m; $\Delta z = 100$ m; $N = L = 200$. The top panel shows the real parts and the bottom panel shows the imaginary parts of the analytical (red line) spectral characteristic and that of the digital filter (blue line).

As an example, Figure (1) presents the plots of spectral characteristics of the analytical and digital filters. We can clearly see in this figure that, for the selected parameters, the spectral characteristics of the digital filter are very close to the analytical curves.

Numerical example of the removal of the sea-layer effect on sea-bottom MCSEM data

The described numerical method of separation of the main part of the field was applied to a 3D synthetic MCSEM data computer simulated for a layered earth model. We have considered the same model, that was analyzed by Fan et al. (2009). The layered model is shown in Figure 2. The target is represented by a 100 m thick horizontal layer with a resistivity of 100 Ohm-m.

The frequency domain EM field was excited by a horizontal 100 m long electric bipole transmitter (shown by a red arrow) located 100 m above an array of the sea-floor receivers (shown by green triangles), with receiver separations equal to 50 m in both the x and y directions. The operating frequency of the transmitter was 0.25 Hz. We used exactly the same parameters of the survey as in Fan et al. (2009), including the same unrealistically dense spacing of the receivers, in order to make a direct comparison between the interferometry method and our approach based on the main part of the anomalous field separation.

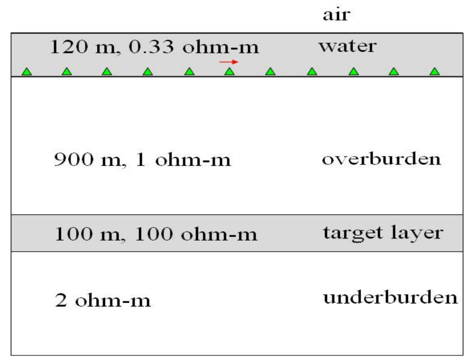

Figure 2: The layered earth model used for testing the method of separation of the main part of the anomalous EM field (after Fan et al., 2009).

The left panels in Figure 3 show maps of the amplitudes of the in-line electric field E_x computed for the layered models with and without a target layer. One can see that there is very little difference between the maps of the fields with and without the target. We observe a similar behavior of the E_x components of the total observed field in amplitude-versus-offset (AVO) plots of these fields for models with and without a target layer (the bottom panel in Figure 4). The red solid lines show the response for the model without a target, while the blue dashed lines present the response for the models with a target. The target produces very little variation of the total field for the offset up to 4 km. There is a very small anomaly in the range of 4 km to 7 km only. One cannot observe any useful effect from the target for the larger offsets, because the field at a large distance from the receiver is dominated by the airwave effect (Fan et al., 2009).

We have applied the corresponding digital filters for the separation of the main part of the anomalous field from the observed synthetic data. Note that in reality we measure the EM field just above the sea floor. However, using the continuity of the horizontal components of the EM field, the vertical components of the electric current, and the vertical component of the magnetic field at the horizontal interface, we can always recalculate the values of the EM field at the top of the sea-bottom sediments, which is required according to the general principles of the main-part separation method.

Indeed, at the horizontal sea bottom we have the following boundary conditions:

$$H_x^{\omega}\big|_{zb}=H_x^{b}\big|_{zb};\quad H_y^{\omega}\big|_{zb}=H_y^{b}\big|_{zb};\quad H_z^{\omega}\big|_{zb}=H_z^{b}\big|_{zb}; \qquad (11)$$

$$E_x^{\omega}\big|_{zb}=E_x^{b}\big|_{zb};\quad E_y^{\omega}\big|_{zb}=E_y^{b}\big|_{zb};\quad \sigma_w E_z^{\omega}\big|_{zb}=\sigma_b E_z^{b}\big|_{zb}. \qquad (12)$$

After transforming the data into the medium with a background resistivity of the overburden, we applied the digital filters for the main-part separation, constructed above. The results of this transformation are shown in the right panels in Figure 3 and the top panel in Figure 4 in the form of the maps and AVO plots of the main part of the anomalous field for models with and without targets. One can see a significant difference in the main parts of the anomalous field between these two models. In other words, the presence of the target is manifested by a strong anomaly in the main part of the field. This result demonstrates that the developed method of separation of the main part of the field can be used for enhancing the effect of the target (a resistive layer associated with an HC reservoir) in the observed MCSEM data.

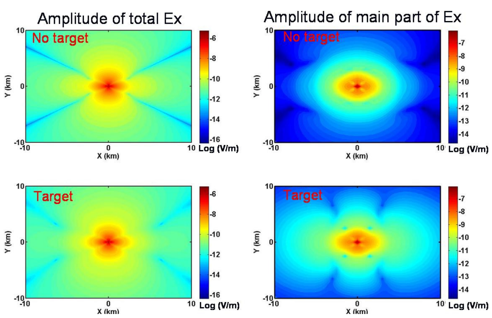

Figure 3: The left panels show maps of the amplitudes of the in-line electric field E_x computed for the layered models with and without a target layer. The right panels present maps of the main part of the anomalous field for models with (bottom panel) and without (top panel) a target.

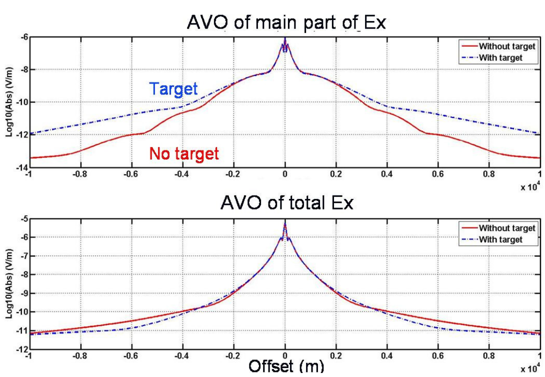

Figure 4: The bottom panel shows the amplitude-versus-offset plots of the in-line electric field E_x, computed for the layered models with a target layer (dashed blue line) and without a target layer (solid red line). The top panel presents the amplitude-versus-offset plots of the main part of the anomalous field for the models with a target layer (dashed blue line) and without a target layer (solid red line).

Conclusions

One of the difficulties in the interpretation of MCSEM survey data in shallow water is related to the airwave effect, which dominates over the observed EM response and masks the anomalous effect of the resistive target. We demonstrate in this paper that this effect can be practically eliminated by a method of separation of the main part of the anomalous field. As a result of this separation, the effect of the air-water interface and the seawater layer is completely removed form the transformed signal.

The numerical method of the main-part separation is based on the application of corresponding digital filters to the observed data. It is shown that the spectral characteristics of this transformation represent a low-frequency filter, which ensures robustness of the numerical algorithm.

Acknowledgments

The authors acknowledge the support of the University of Utah Consortium for Electromagnetic Modeling and Inversion (CEMI).

EDITED REFERENCES

Note: This reference list is a copy-edited version of the reference list submitted by the author. Reference lists for the 2010 SEG Technical Program Expanded Abstracts have been copy edited so that references provided with the online metadata for each paper will achieve a high degree of linking to cited sources that appear on the Web.

REFERENCES

Amundsen, L., L. Løseth, R. Mittet, S. Ellingsrud, and B. Ursin, 2006, Decomposition of electromagnetic fields into upgoing and downgoing components: Geophysics, **71**, G211–G223. doi:10.1190/1.2245468

Berdichevsky, M. N., and M. S. Zhdanov, 1984, Advanced theory of deep geomagnetic sounding: Elsevier.

Fan, Y., R. Snieder, and J. Singer, 2009, 3-D Controlled Source Electromagnetic (CSEM) interferometry by multi-dimensional deconvolution: 79th Annual International Meeting, SEG, Expanded Abstracts.

Schuster, G. T., 2009, Seismic interferometry: Cambridge University Press.

Slob, E., D. Draganov, and K. Wapenaar, 2007, Interferometric electromagnetic Greens functions representations using propagation invariants: Geophysical Journal International, **169**, no. 1, 60–80, doi:10.1111/j.1365-246X.2006.03296.x.

Snieder, R., 2006, Retrieving the Greens function of the diffusion equation from the response to a random forcing: Physics Review E, **74**, 046-620.

Wapenaar, K., E. Slob, and R. Snieder, 2008, Seismic and electromagnetic controlled-source interferometry in dissipative media: Geophysical Prospecting, **56**, no. 3, 419–434, doi:10.1111/j.1365-2478.2007.00686.x.

Zhdanov, M. S., 1988, Integral transforms in geophysics: Springer-Verlag.

Zhdanov, M. S., and S. Wang, 2009a, Foundations of the method of EM field separation into upgoing and downgoing parts and its application to MCSEM data, *in* J. Kasahara, V. Korneev, and M. S. Zhdanov, eds., Active Geophysical Monitoring: Elsevier, 351-380.

Zhdanov, M. S., and S. Wang, 2009b, Foundations of the method of EM field separation into upgoing and downgoing parts and its application to MCSEM data: 79th Annual International Meeting, SEG, Expanded Abstracts.

Zhdanova, O. N., and M. S. Zhdanov, 1999, Methods for the analysis and interpretation of the sea floor electromagnetic fields: Deep Electromagnetic Exploration: Springer-Verlag, Narosa Publishing House.